Check for updates

Original Research

Fibrin Scaffold With Concentrated Growth Factor and Stromal Vascular Fraction

A Novel Approach for Repairing Chronic Rotator Cuff Tears in a Rabbit Model

Ahmet Keskin,*† MD, Hilal Kabadayi Ensarioglu,‡ PhD, Hafize Seda Vatansever,§|| PhD, Serhat Gurbuz,† MD, Yasin Guler,† MD, Bülent Karslioğlu,† MD, Samed Ozer,¶ MD, Yunus Imren,# MD, Ergun Bozdag,** PhD, Kerem Bilsel,†† MD, and Suleyman Semih Dedeoglu,# MD

Investigation performed at Acibadem Mehmet Ali Aydinlar University Experimental Animals Application and Research Center, Istanbul, Turkey

Background: Rotator cuff tears (RCTs) represent a significant challenge in orthopaedic care, particularly in chronic cases where tendon healing is suboptimal. Novel biological therapies such as concentrated growth factor (CGF) and stromal vascular fraction (SVF) offer promising solutions for enhanced tendon repair.

Hypothesis: This study hypothesized that a fibrin scaffold enriched with CGF and SVF would improve tendon healing by reducing fatty degeneration, increasing vascularization, and enhancing biomechanical properties in a chronic RCT rabbit model.

Study Design: Controlled laboratory study.

Methods: A chronic RCT model was developed in the subscapularis tendon of 28 male New Zealand rabbits. In the first phase (week 0), the chronic injury model was created surgically. At week 6, in addition to the transosseous repair technique, biological materials were applied into the bone tunnel in each group as follows: hydrogel (group 1), fibrin gel with CGF (group 2), CGF+SVF–enriched fibrin scaffold (group 3), and no repair (group 4). At week 12, animals were euthanized, and samples were collected for macroscopic, histological, immunohistochemical, and biomechanical analysis.

Results: Group 3 demonstrated a superior result. Fatty degeneration was significantly lower in group 3 compared with group 1 (P = .045). Vascularization and cellularity scores were highest in group 3 (3.7 ± 0.5 and 3.6 ± 0.5, respectively), significantly greater than group 1 (1.4 ± 0.5 and 1.3 ± 0.5, respectively) (P = .024 and P = .004, respectively). Collagen fiber continuity and regularity scores were 3.7 ± 0.5 and 3.6 ± 0.5 in group 3, respectively, significantly better than group 1 (1.4 ± 0.5 and 1.3 ± 0.5, respectively) (P = .006 and P = .003, respectively). Biomechanical testing revealed the highest tensile strength in group 3 (116.14 ± 8.49 N; $P < .001$). Midsubstance tears, indicating robust healing, were observed in 85.7% of tendons in group 3 compared with 28.6% in group 1 (P = .002). Notably, group 3 also demonstrated superior outcomes compared with group 2, with significantly greater tensile strength (116.14 ± 8.49 N vs 100 ± 6.85 N; $P < .001$) and improved histological parameters including reduced fatty degeneration, and increased vascularization and collagen fiber regularity.

Conclusion: The inclusion of CGF and SVF in fibrin scaffolds significantly enhances tendon healing in chronic RCTs, outperforming the use of CGF alone. This combined biological approach offers a promising therapeutic strategy to optimize tendon repair outcomes.

Clinical Relevance: These findings support the clinical potential of CGF and SVF in improving repair outcomes in chronic RCT cases in sports medicine.

Keywords: rotator cuff tears; concentrated growth factor; stromal vascular fraction; rabbit model

The Orthopaedic Journal of Sports Medicine, 13(10), 23259671251366686
DOI: 10.1177/23259671251366686
© The Author(s) 2025

Rotator cuff (RC) tears (RCTs) are a significant cause of pain and functional impairment in orthopaedic practice, particularly when they become chronic. Although surgical

This open-access article is published and distributed under the Creative Commons Attribution - NonCommercial - No Derivatives License (https://creativecommons.org/licenses/by-nc-nd/4.0/), which permits the noncommercial use, distribution, and reproduction of the article in any medium, provided the original author and source are credited. You may not alter, transform, or build upon this article without the permission of the Author(s). For article reuse guidelines, please visit SAGE's website at http://www.sagepub.com/journals-permissions.

repair techniques are widely used, the management of chronic RCT remains a challenge, often leading to suboptimal healing and persistent dysfunction.[28]

In recent years, biological therapies have gained attention for their potential to enhance tendon repair by promoting regenerative processes. Among these, approaches such as platelet-rich plasma (PRP), bone marrow aspirate concentrate, mesenchymal stem cells, and stromal vascular fraction (SVF) have shown promise in musculoskeletal medicine.[4,8,33] Despite these advancements, the repair of chronic RCT remains complex due to the persistent degenerative changes and poor vascularity associated with these injuries.

Concentrated growth factor (CGF), a third-generation platelet concentrate, has emerged as a novel therapeutic tool, known for its ability to accelerate tissue healing. SVF, derived from adipose tissue, contains a mixture of mesenchymal stem cells, endothelial progenitor cells, and macrophage precursors, all of which contribute to tissue regeneration.[13,15] Studies have shown that SVF can improve tendon-bone healing and reduce fat infiltration, which is critical for enhancing tendon repair outcomes.[32] Furthermore, adipose-derived stem cells (ADSCs), a component of SVF, have been demonstrated to mitigate ischemic damage, thereby improving cell survival in injured tendon and muscle tissues.[40]

The rabbit subscapularis muscle and tendon exhibit notable anatomic and biomechanical similarities to the human supraspinatus tendon, particularly with respect to origin, insertion, and neural innervation. The unique anatomic structure of the rabbit subscapularis tendon, which passes through a bony tunnel before attaching to the humerus, closely parallels the human supraspinatus tendon traversing the subacromial space.[14] This anatomic congruence makes the rabbit model a reliable tool for studying the pathophysiology of chronic RCT and evaluating tendon healing interventions.[14]

Despite the promising results of PRP and mesenchymal stem cell therapies, an optimal treatment strategy for chronic RC tendinopathy has yet to be established.[1] To overcome the limitations of existing regenerative therapies for chronic RCT, this study evaluated the combined application of CGF and SVF. These agents were selected for their potential to synergistically enhance tendon healing by promoting vascularization, cellular proliferation, and collagen organization. In contrast to traditional PRP therapies, CGF provides a denser scaffold enriched with regenerative proteins and cellular components.[9,27] SVF complements CGF by contributing a diverse array of mesenchymal stem cells, endothelial progenitor cells, and immunomodulatory factors.[15,32,45] Despite encouraging preclinical findings, the composition of CGF and SVF and their precise mechanisms of action remain insufficiently characterized. This study addresses these gaps by quantifying key components of CGF and SVF in a rabbit model of chronic RCT, while employing comprehensive macroscopic, histological, immunohistochemical, and biomechanical analyses to elucidate their therapeutic potential.

METHODS

Ethics committee approval was obtained from the Acibadem Mehmet Ali Aydinlar University Animal Experiments local ethics committee, and the animal experiments were conducted at the Acibadem Mehmet Ali Aydinlar University Experimental Animals Application and Research Center, accredited by the Association for Assessment and Accreditation of Laboratory Animal Care International.

Determination of Sample Size

Power analysis was conducted to ensure adequate sample size for detecting significant differences in both histological and biomechanical evaluations. For the histological examination, a minimum of 4 animals per group was needed to achieve 80% power with a 5% margin of error, an effect size of 1.059, and a SD of 15.[3,39] For biomechanical evaluation, to achieve 80% power with a 5% margin of error, an effect size of 0.70, and an SD of 115, a minimum of 7 animals per group was required.[22,36] Consequently, 7 rabbits were assigned to each group in the study.

The study involved 28 male New Zealand rabbits, each weighing between 3 and 4 kg and approximately 24 weeks old. The rabbits were maintained under standard laboratory conditions (12-hour dark/light cycle, room temperature 22°C, and humidity 50%-60%), with each rabbit housed individually in a cage and provided with free access to food and water. A 10-day acclimatization period was

*Address correspondence to Ahmet Keskin, MD, Department of Orthopaedics and Traumatology, Metin Sabancı Bone Diseases Training and Research Hospital, Rumeli Hisarı Street, No. 62, Sariyer 34470 Istanbul, Turkey (email: drkeskinahmet@gmail.com).

†Department of Orthopaedics and Traumatology, Metin Sabanci Bone Diseases Training and Research Hospital, Istanbul, Turkey.

‡Department of Histology and Embryology, Faculty of Medicine, Izmir Bakircay University, Izmir, Turkey.

§Department of Histology and Embryology, Faculty of Medicine, Manisa Celal Bayar University, Manisa, Turkey.

‖DESAM Research Institute, Near East University, Mersin, Turkey.

¶Department of Physiology, Acibadem Mehmet Ali Aydinlar University, Istanbul, Turkey.

#Department of Orthopaedics and Traumatology, Istinye University, Liv Hospital Vadistanbul Istanbul, Turkey.

**Faculty of Mechanical Engineering, Istanbul Technical University, Istanbul, Turkey.

††Department of Orthopaedics and Traumatology, Faculty of Medicine, Acibadem Mehmet Ali Aydinlar University, Istanbul, Turkey.

Final revision submitted April 12, 2025; accepted May 29, 2025.

The authors declared that there are no conflicts of interest in the authorship and publication of this contribution. AOSSM checks author disclosures against the Open Payments Database (OPD). AOSSM has not conducted an independent investigation on the OPD and disclaims any liability or responsibility relating thereto.

Ethical approval for this study was obtained from the Acibadem Mehmet Ali Aydinlar University Animal Experiments local ethics committee (Date/No.: November 24, 2020/HDK-2020/52).

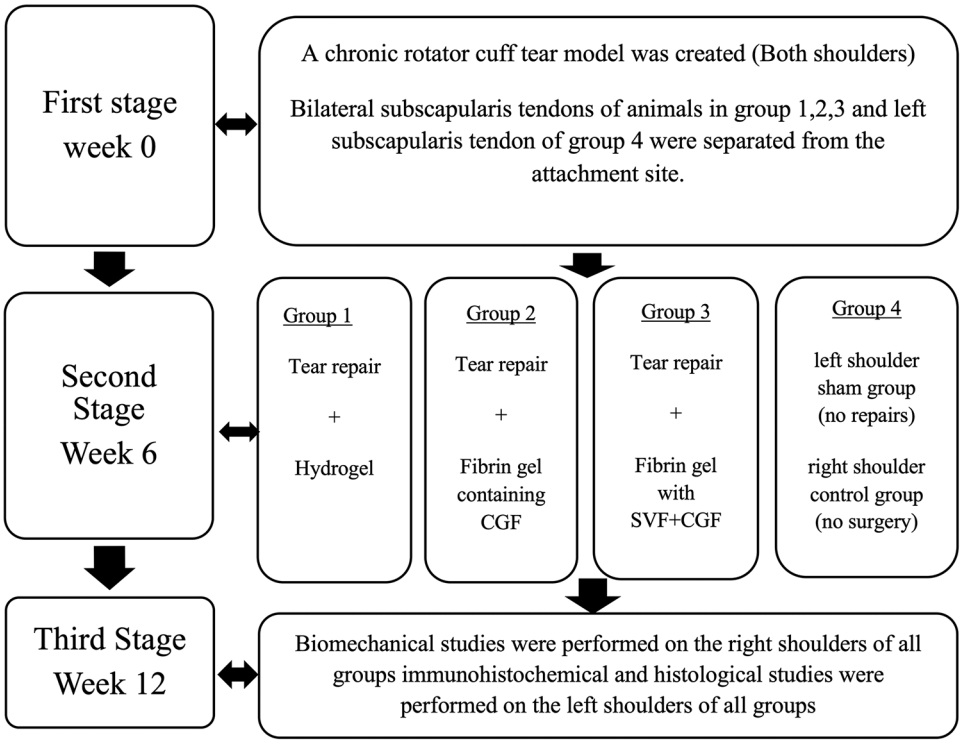

Figure 1. Flowchart of the study design. CGF, concentrated growth factor; SVF, stromal vascular fraction.

observed before the rabbits were randomly allocated into 4 groups based on the repair procedure to be implemented.

Study Design and Experimental Groups

All experimental procedures were conducted bilaterally under general anesthesia by a single surgeon (A.K.). The general anesthesia protocol included intramuscular administration of ketamine (35-40 mg/kg) and xylazine (3-5 mg/kg), as outlined in the literature.[31] For infection prophylaxis, intramuscular gentamicin (3 mg/kg) was administered.

The study was performed in 3 stages, as depicted in Figure 1.

Chronic RCT Model Creation. In the first stage, the bilateral subscapularis tendons in groups 1, 2, and 3, and the left subscapularis tendon in group 4, were detached from their humeral attachment site to create a chronic tear model following the technique described by Oh et al.[25]

After anesthesia, the rabbits were positioned laterally, and measures were taken to restrict involuntary movements. The shoulders were shaved, and a longitudinal skin incision of approximately 3 cm was made using the deltopectoral approach to expose the subscapularis tendon. A full-thickness cut was performed at the tendon insertion site on the humerus. To prevent adhesion of the ruptured tendon tip to surrounding soft tissues, an 8 mm–diameter and 10 mm–length silicone Penrose drain was wrapped around the area, establishing a chronic rupture model (Figure 2). After the procedure, the fascia and skin were sutured, and the rabbits were allowed 6 weeks for chronic changes to develop in the RC tendons.[12,29,37]

In the first stage, a chronic RCT model was surgically induced in the bilateral subscapularis tendons of groups 1, 2, and 3. For group 4, the left subscapularis tendon was surgically detached to establish a sham group, while the right shoulder remained intact as an untreated control. The left shoulders in group 4 underwent the described surgical procedure to induce chronic tendon injury but received no subsequent repair. This sham group was included to provide a reference for histological and immunohistochemical analysis, enabling the assessment of unaltered chronic degenerative changes over the 12-week study period.

The right shoulders of group 4 animals were preserved as native controls, undergoing no surgical intervention. These intact shoulders served as macroscopic baselines and biomechanical references for evaluating tendon integrity, tensile strength, and healing outcomes in the repaired groups 1, 2, and 3. Thus, group 4 effectively provided both a pathological control (left shoulder, sham) and a normal physiological and biomechanical reference (right shoulder, control).

Repair and Treatment Application. In the second stage of the study (sixth week), CGF and SVF preparations were derived from the blood and adipose tissue of the rabbits after anesthesia and prophylaxis procedures were completed. A sterile Vacuette was used to collect 9 mL of blood from each rabbit in groups 2 and 3. Centrifugation of these tubes at 69 relative centrifugal force (RCF, or G-force) for 2 minutes, 54 G-force for 4 minutes, 69 G-force for 4 minutes, and 85 G-force for 3 minutes with gradual deceleration produced 3

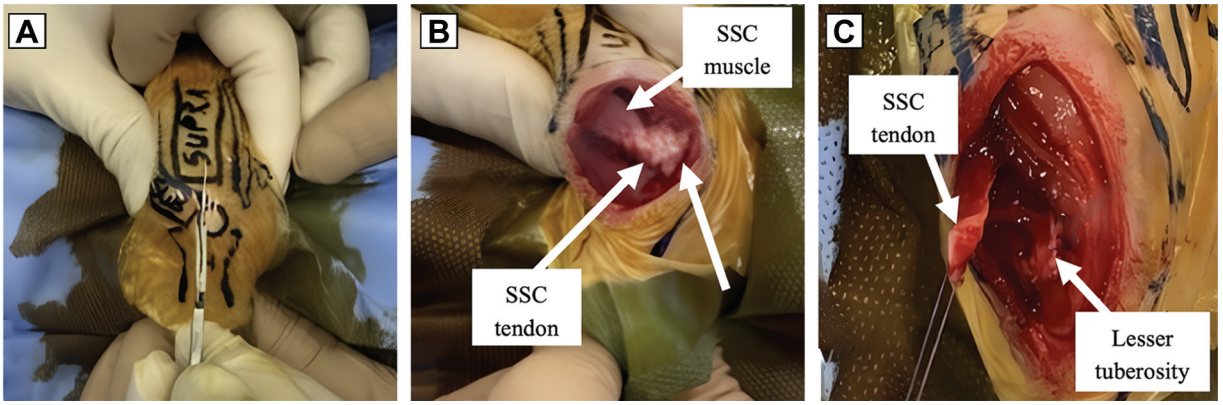

Figure 2. Creation of the chronic tear model in the first stage. (A) Longitudinal incision. (B) Exposure of the subscapularis (SSC) tendon. (C) Full-thickness incision from the insertion part of the SSC tendon.

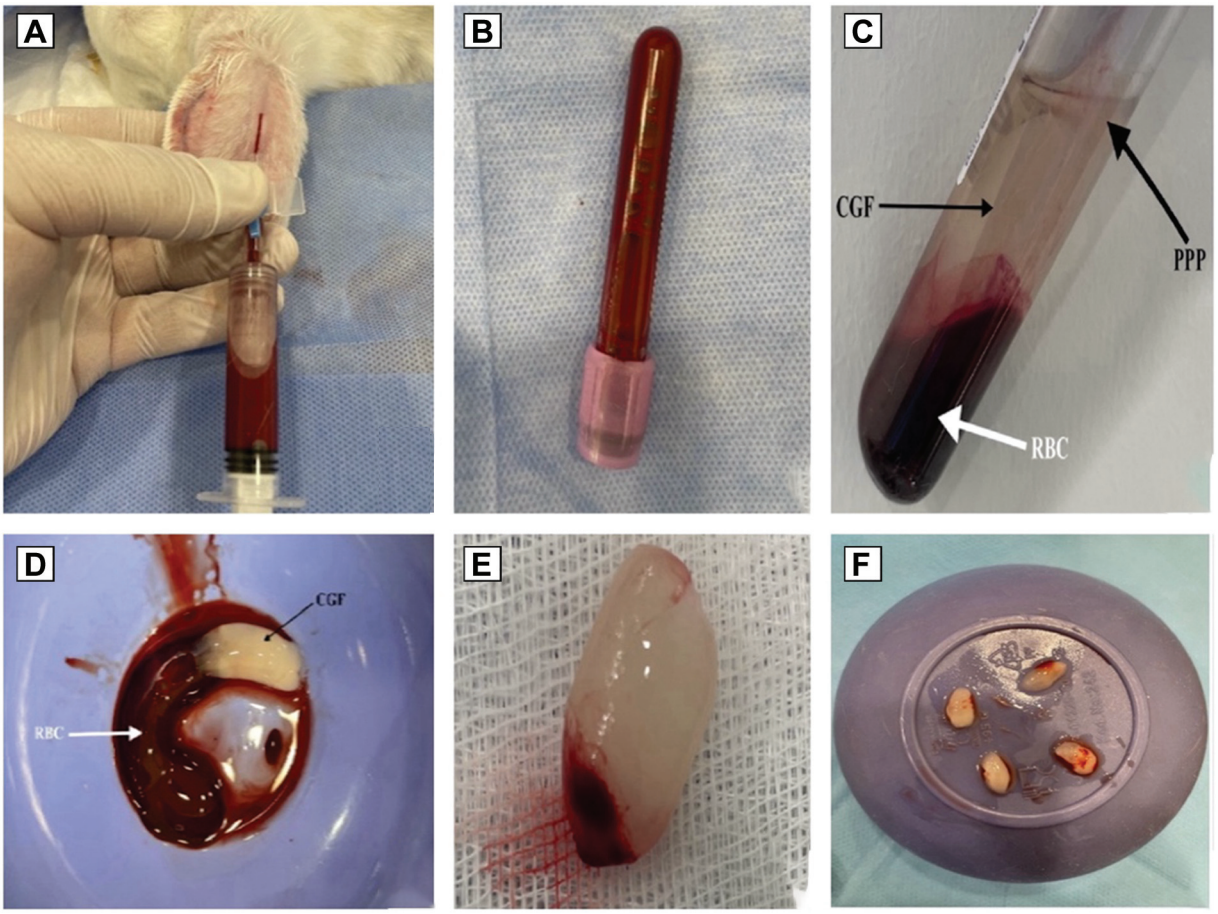

Figure 3. Methods applied for CGF isolation. (A) Collection of 10 cc of blood from each rabbit; (B) collection in a sterile manner using Vacuette; (C) layers formed after centrifugation; (D) fibrin block with red interface obtained after storage at −80°C; (E) obtained CGF; and (F) chopped CGF pieces. CGF, concentrated growth factor; PPP, platelet-poor plasma, acellular plasma; RBC, red blood cell.

blood fractions. The intermediate phase, known as CGF, was identified as a dense fibrin block containing white blood cells and stem cells[27] (Figure 3).

Before the surgical procedures on rabbits in group 3, a transverse 3-cm incision was made in the midline suprapubic region to expose the inguinal fat pad for

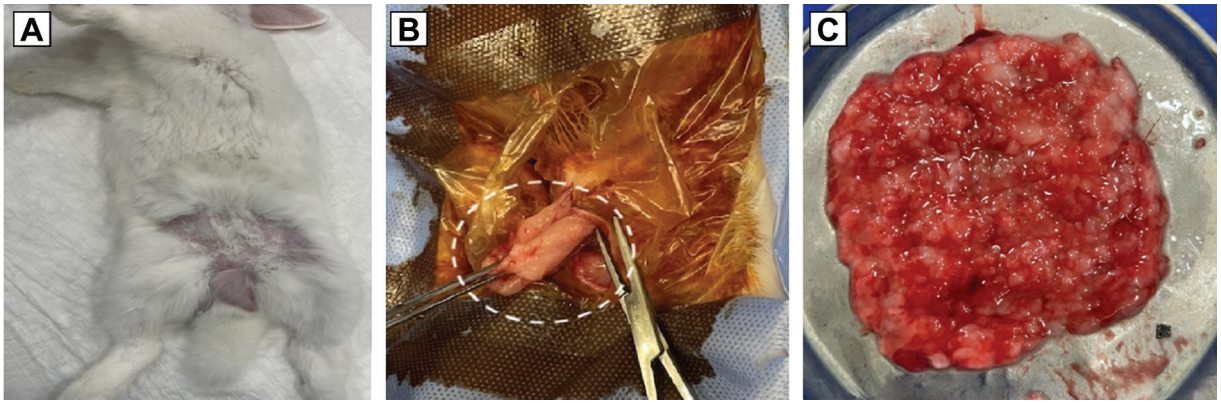

Figure 4. Stromal vascular fraction isolation preparation stages. (A) Suprapubic midline alignment. (B) Exposure of 5 ml of pure fat tissue (dotted circle: inguinal fat pad). (C) Mechanical dissection of the obtained fat tissue into pieces.

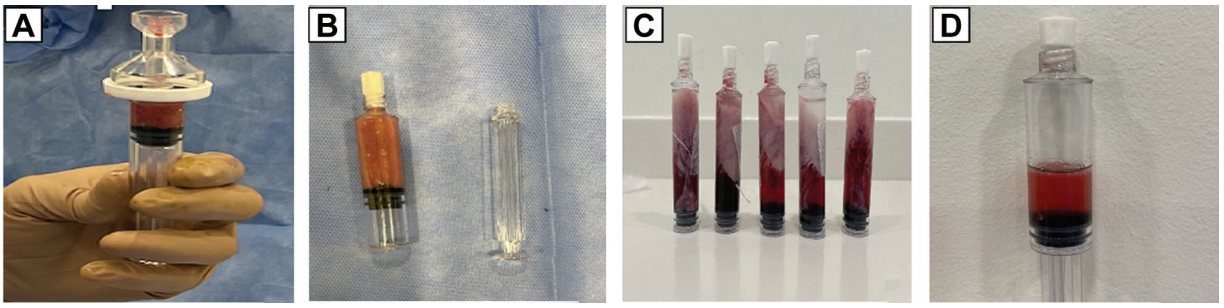

Figure 5. Stromal vascular fraction (SVF) isolation enzymatic and centrifugation steps. (A) Collection of fat tissue pieces into the tube and washing with phosphate buffered saline. (B) Centrifugation of obtained material. (C) Material obtained postcentrifugation at 13 G-force after resting at room temperature. (D) SVF separation from adipocytes and cell debris.

subcutaneous adipose tissue harvesting. The fat pad was then excised, and the SVF was isolated using the protocol described by Zuk et al[45] (Figures 4 and 5). In addition to the surgical repair in group 3, SVF was injected into the CGF fibrin block to create a fibrin scaffold (Figure 6).

The Penrose drain was removed under aseptic conditions, and the fibrocartilaginous stump remaining in the lesser tuberosity was thoroughly cleaned for the transosseous repair technique. A bone pit measuring 8 mm in length, 2 mm in width, and 2 mm in depth was created in the lesser tuberosity using a high-speed burr. In the proximal lateral humerus, 2 drill holes with a diameter of 0.8 mm were made. The substances allocated for each group (group 1, hydrogel; group 2, CGF fibrin gel; group 3, CGF fibrin gel + SVF) were placed in these tunnels (Figures 7 and 8). The hydrogel group (group 1) was incorporated as a baseline comparator to evaluate the incremental effects of CGF and CGF+SVF scaffolds. Hydrogel serves as a commonly used carrier medium in tissue engineering, providing a standard reference for assessing the efficacy of the experimental scaffolds. Subsequently, the torn subscapularis tendons were sutured to their anatomic position using 3-0 Prolene (Ethicon) with 2 horizontal sutures, and the hydrogel/fibrin gel was secured between the tendon end and the bone by attaching

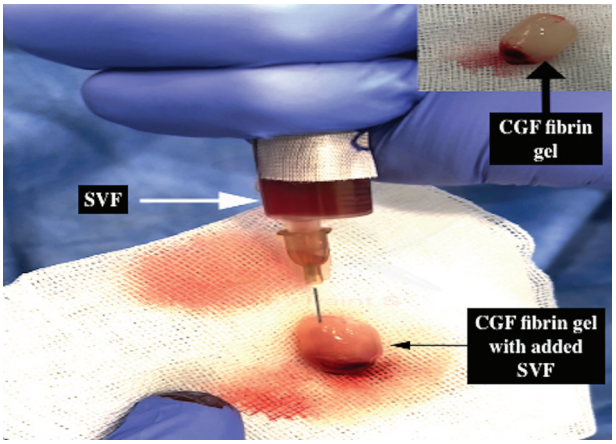

Figure 6. Obtaining of fibrin scaffold by injecting stromal vascular fraction (SVF) into concentrated growth factor (CGF).

a suture to the humeral cortex. The surgical incisions were closed in layers with 4-0 nylon sutures. No intervention was performed in group 4 during the second stage.

During both the first and the second stages, prophylactic measures were taken to prevent surgical-site infections,

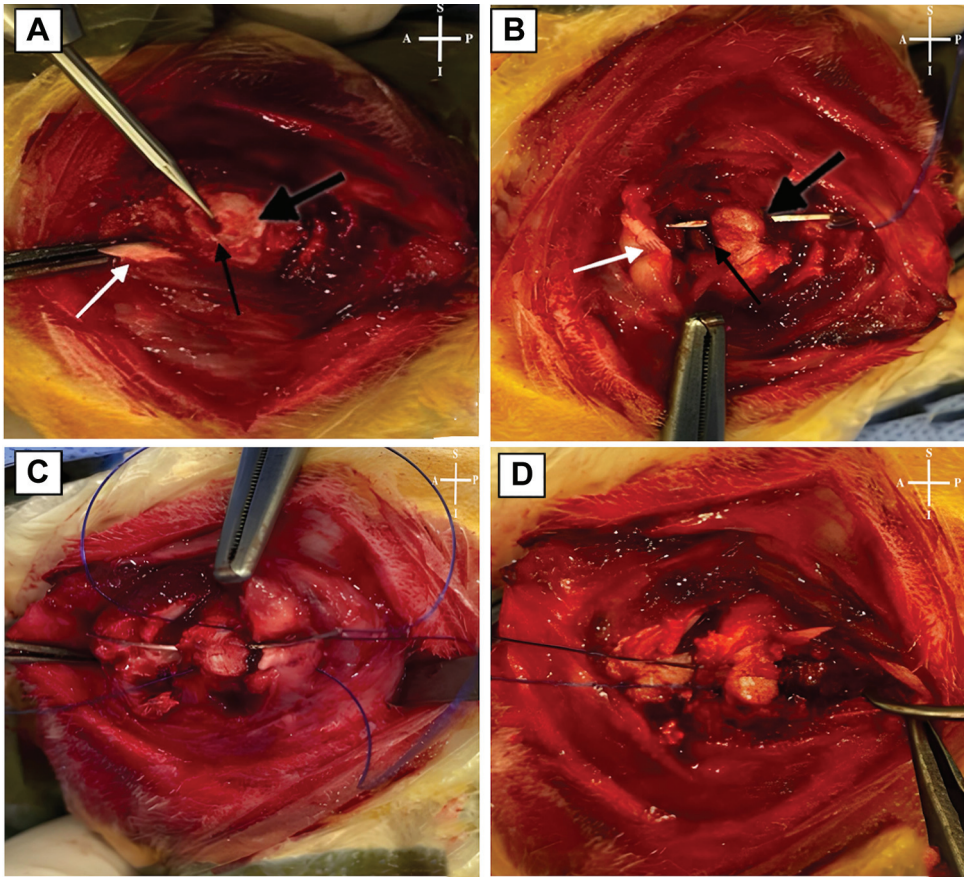

Figure 7. Surgical technique for chronic subscapularis (SSC) tendon repair in rabbit model. Panels illustrate step-by-step surgical procedures. (A) Tunneling of the lesser tuberosity using a high-speed microburr to create a bone tunnel for transosseous fixation (white arrow indicates the SSC tendon prepared for repair; black thick arrow indicates the lateral wall of the proximal humerus; black thin arrow indicates the bone tunnel created at the lesser tuberosity). (B) Passing of the transosseous repair suture through the bone tunnel and tendon (white arrow indicates the SSC tendon prepared for repair; black thick arrow indicates the lateral wall of the proximal humerus; black thin arrow indicates the bone tunnel created at the lesser tuberosity). (C) Transosseous suture placement completed. The blue suture loops represent the sutures passed through the prepared tunnel and tendon, positioned ready for securing. (D) Completed transosseous repair of the SSC tendon. The repaired SSC tendon is shown clearly approximated to the bone with the transosseous suture technique. A, anterior; I, inferior; P, posterior; S, superior.

pain, and surgical stress. Gentamicin was administered intramuscularly at 3 mg/kg for 3 days, buprenorphine subcutaneously at 0.02 mg/kg for 2 days, and 100 cc of isotonic fluid was administered to prevent surgical stress postoperatively. The limbs were not immobilized postoperatively, but a collar was fitted to prevent self-injury to the operative site. No rabbits died during or after surgery. One rabbit in group 2 developed a superficial infection, treated with antibiotics, without requiring debridement. Another rabbit in group 3 developed an abscess in the area where the inguinal fat pad was removed, which was treated with debridement and healed without complications.

Euthanasia and Sample Collection. In the third stage (12th week), the rabbits were euthanized using carbon dioxide inhalation per standard anesthesia protocol. The right shoulders were used for biomechanical examination and macroscopic finding comparison, while the left shoulders were designated for histological and immunohistochemical analysis.

Histological and Immunohistochemical Analysis

Histological and immunohistochemical evaluations were performed at the Department of Histology and Embryology, Faculty of Medicine, Manisa Celal Bayar University. To eliminate researcher bias and ensure objectivity, all histological assessments were conducted independently by 2 histologists (H.K.E and H.S.V.), each of whom was blinded to the group allocations. The tissue sections were randomly assigned numbers, and their original identities remained concealed throughout the evaluation process. Following completion of the assessments, the true identities of each section were revealed by decoding the random number assignments.

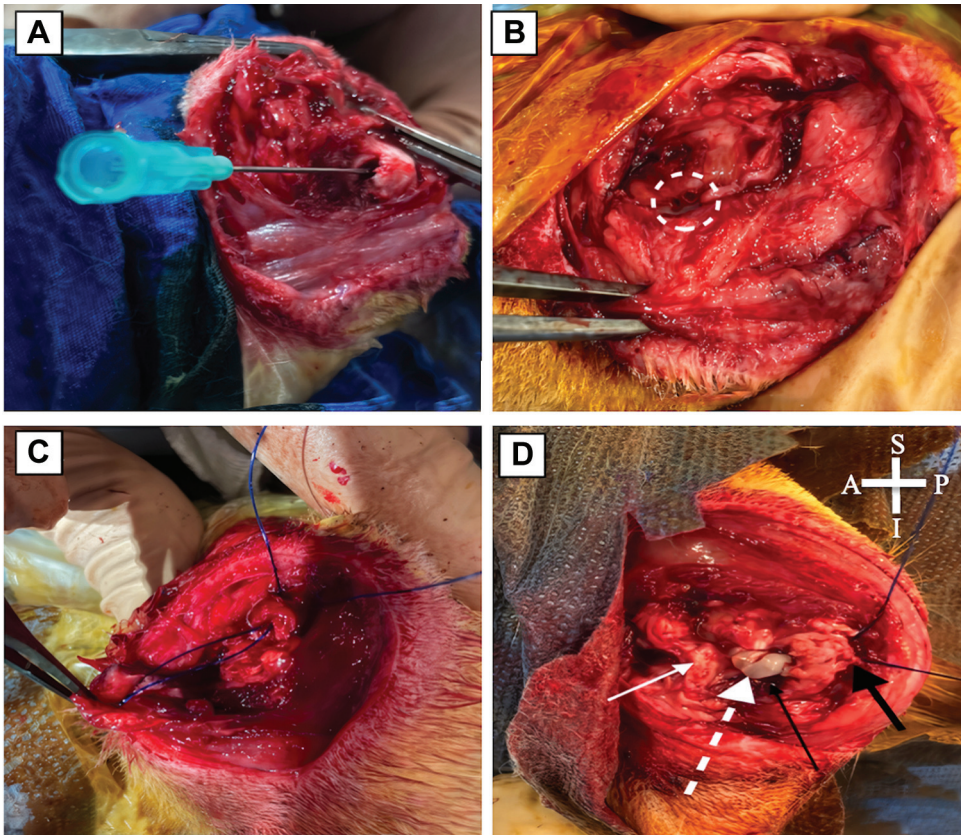

Figure 8. Surgical technique of second-stage tendon repair in rabbits from groups 2 and 3, demonstrating the transosseous repair method with biological augmentation. (A) Creation of bone tunnel (indicated by needle tip) in the lesser tuberosity for biologic substances. (B) Preparation of transosseous suture holes (white dashed circles) in the lateral wall of the proximal humerus. (C) Transosseous passage of repair sutures through the prepared bone tunnels in the lesser tuberosity and lateral humeral wall, clearly demonstrating suture configuration. (D) Completed transosseous tendon repair with biological augmentation using CGF+SVF fibrin scaffold (white dashed arrow), positioned between the subscapularis tendon (white thin arrow) and the lateral humeral wall (black thick arrow). The black thin arrow indicates the bone tunnel at the lesser tuberosity, demonstrating precise suture anchor placement.). A, anterior; CGF, concentrated growth factor; I, inferior; P, posterior; S, superior; SVF, stromal vascular fraction.

Tissue samples were systematically harvested from the subscapularis muscle's attachment site at the lesser tuberosity using a coronal plane orientation. Each specimen measured 10 mm along the mediolateral axis (parallel to the tendon's longitudinal collagen alignment) and 3 mm in the superoinferior dimension to ensure inclusion of the muscle belly, midsubstance tendon, and tendon-bone interface to standardize anatomic coverage. Following excision and sample collection, samples underwent fixation in 10% neutral buffered formalin (15512-2.5L-R; Sigma Aldrich) for 24 to 48 hours and decalcification in 0.02 M Etilendiamintetraasetik acid (EDTA) (E6511; Sigma Aldrich) for 8 weeks with weekly solution renewal. For paraffin embedding, tissues were rinsed under running tap water for 12 hours, dehydrated through a graded ethanol series (30 minutes each in 60%, 70%, 80%, 95%, and absolute ethanol), cleared in xylene and infiltrated with paraffin (Figure 9).

Embedded blocks were sectioned coronally at 5-μm thickness using a rotary microtome (RM 2135; Leica), ensuring preservation of collagen fiber orientation for histological and immunohistochemical analyses. For immunohistochemical analysis, collagen types I and III, vascular endothelial growth factor (VEGF), proliferating cell nuclear antigen (PCNA), and cluster of differentiation 31 (CD31; also known as platelet endothelial cell adhesion molecule) were evaluated using the indirect immunoperoxidase technique.

Histological Analysis

Hematoxylin-eosin (H&E) staining: sections were deparaffinized, rehydrated, and stained with hematoxylin (01562E and 01602E; Surgipath) for 5 minutes and eosin for 1 minute.

Oil Red O staining: lipids were visualized by staining sections with Oil Red O (SC-203749A; Santa Cruz Biotechnology) for 15 minutes, followed by hematoxylin counterstaining. Lipids appeared red, and nuclei were blue.

Masson trichrome staining: samples were stained with Weigert hematoxylin, ponceau acid fuchsin, phosphotungstic acid, and methyl blue. This resulted in blue-black nuclei, red cytoplasm, and blue collagen fibers.

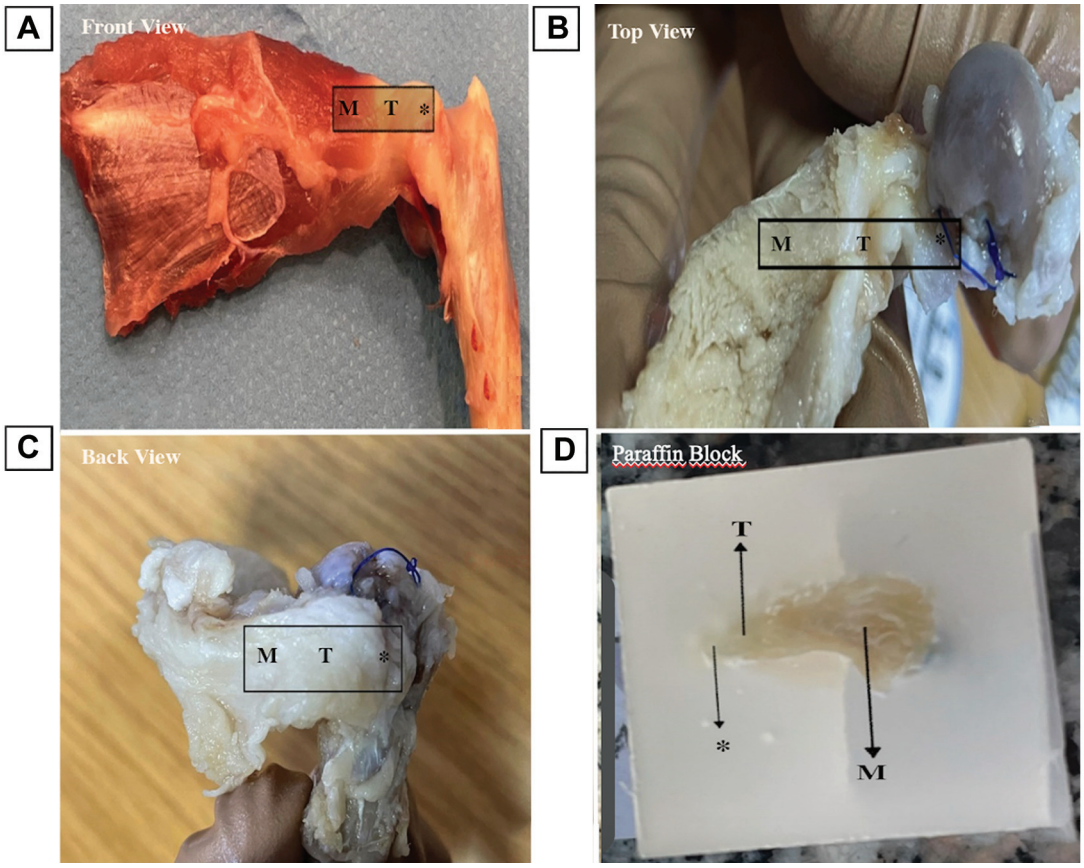

Figure 9. Representative demonstration of systematic preparation stages and tissue orientation for histological analysis. (A) Front view showing harvested specimen from subscapularis muscle attachment at lesser tuberosity. (B) Top view illustrating tissue orientation along the mediolateral axis. (C) Posterior view confirming standardized anatomic coverage with clear visualization. (D) Paraffin-embedded tissue block, oriented to maintain the integrity of muscle (M), tendon (T), and tendon-bone interface (*).

Immunohistochemical Analysis

Beyond H&E and Masson trichrome staining, the study utilized second harmonic generation microscopy for collagen orientation analysis and immunofluorescence to quantify cellular markers such as PCNA and VEGF. After deparaffinization and rehydration, antigen retrieval was conducted using 0.5% trypsin at 37°C. Endogenous peroxidase was blocked with 3% hydrogen peroxide. Primary antibodies for VEGF, type III collagen, PCNA, and CD31 were incubated with sections, followed by a biotin-labeled secondary antibody (Histostain Plus Bulk Kit; Invitrogen) and streptavidin application. Diaminobenzidine was used for detection, and Mayer hematoxylin was applied for counterstaining. Negative controls were performed by omitting the primary antibody. Staining intensity was graded as negative (–), weak (+), moderate (++), or strong (+++) based on the intensity of immunoreactivity. A negative (–) score was assigned when no detectable immunostaining was observed in the tissue sections.

Histological Analysis—Histopathological Scoring Systems

The data were graded semiquantitatively using 4 grades (1, 2, 3, and 4) as described in the literature.[7] Vascularity and cellularity were graded as absent or minimal (grade 1), mild (grade 2), moderate (grade 3), or severe/pronounced (grade 4). The continuity and orientation (parallel, perpendicular) of collagen fibers were evaluated by calculating percentages (grade 1, <25%; grade 2, 25%-≤50%; grade 3, >50%-75%; and grade 4, >75%). For fatty degeneration assessment, each section was blindly analyzed by 2 independent histologists (H.K.E and H.S.V.), scanning 3 separate areas per section in duplicate. For quantitative analysis, the fatty degeneration rate was calculated by averaging the 3 measured field values. Oil Red O staining resulted in 4 grades according to the percentage of stained area (grade 1, <25% fatty degeneration and weak staining; grade 2, 25%-≤50% degeneration and weak-moderate staining; grade 3, >50%-75% degeneration and medium-strong staining; grade 4, >75% degeneration and strong staining).

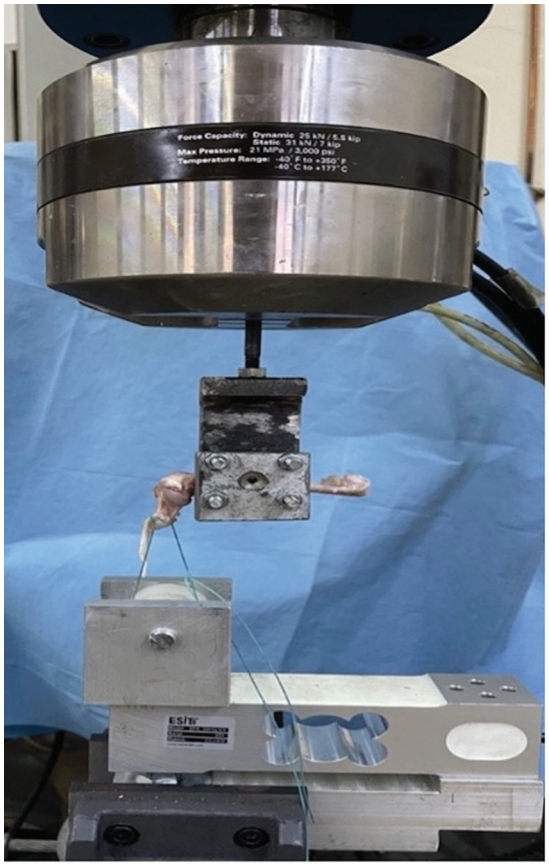

Figure 10. MTS 858 Mini Bionix II device used for mechanical testing. The coding of the load cell manufacturer indicates ESIT SPA 100 kg (maximal force value), serial number (S/N) 824.

Biomechanical Analysis

Biomechanical tests were conducted at the Istanbul Technical University's Biomechanics and Strength Laboratory. Samples were preserved in saline-moistened gauze at −80°C and thawed at room temperature (25°C; 70% humidity) for 12 hours before testing. Bone fixation was achieved using a custom-designed apparatus attached to the upper jaw of a universal tension device (MTS 858 Mini Bionix II; Servohydraulic Test Systems). The tendons were secured to the load cell of the suture thread (ESIT SPA 100 kg; serial No. 824). To prevent suture thread rupture due to excessive force transmission, the thread passing through the tendon were wrapped around a cylindrical spool attached to the load cell, which maintained friction and distributed the load evenly. This setup minimized the direct tensile load on the thread itself, thereby ensuring that the measured force accurately reflected the tensile strength of the tendon-bone interface (Figure 10).

Initial system stabilization was conducted by applying an axial tensile force ranging from 0 N to 45 N at a frequency of 1.0 Hz for 15 cycles. Following stabilization, tensile testing was performed at 1 mm/sec until rupture or separation from the bone. The force value and damage mode were recorded. Data from the force measurements were analyzed using MATLAB 2018 software (MathWorks).

Statistical Analysis

Statistical analyses were conducted using SPSS Version 23.0 software (SPSS Inc). To evaluate differences between groups in histological staining, biomechanical testing, and histological examinations, the Kruskal-Wallis test was employed. For paired group comparisons, the Pearson chi-square test was utilized. A P value of $<.05$ was considered statistically significant, indicating a meaningful difference between the groups.

RESULTS

Macroscopic Findings

Group 3 exhibited significantly less scar tissue formation compared with group 1, with macroscopic appearance closely resembling intact tendon-bone interfaces observed in group 4 (Figure 11).

Histological Evaluation

Oil Red O staining, indicating lipid presence, was most pronounced in group 4, followed by groups 1, 2, and 3, respectively (Figure 12). Fatty degeneration was significantly lower in group 3, which received the SVF+CGF fibrin scaffold combination, compared with the other groups (P = .045). Blood vessel density, an indicator of vascularization, was lowest in group 1 and highest in group 3 (P = .024). Cellularity was also highest in group 3 (P = .004). At the tendon-bone interface, the proportion of collagen fibers was substantially increased in group 3, with better collagen organization than in group 1. Longitudinally oriented collagen fibers were seen across all groups; however, compared with group 1, group 3 exhibited significantly better collagen fiber continuity (P = .006) and regularity (P = .003) (Tables 1 and 2). Collagen fibers at the tendon-bone interface in the CGF-treated groups appeared relatively more perpendicular to the bone (Figure 12, Tables 1 and 2).

Masson trichrome staining in group 3 showed higher collagen density and better collagen organization than in the other groups (Figure 13).

The ratios of vascularity and cellularity assessed after H&E staining were higher in group 3 (Figure 14).

Immunohistochemistry

Type I collagen immunoreactivity was strongest (+++) in group 3 and weakest in group 1 (+/++), with group 4 showing no immunoreactivity (Figure 15). Type III collagen immunoreactivity was strongly positive (+++) in group 1, moderate (++) in groups 2 and 3, and negative in group 4 (Figure 15). PCNA-positive cells, indicating proliferation, were mainly observed in the repair tissue, showing moderate (++) immunoreactivity in groups 1 and 2, strong (+++)

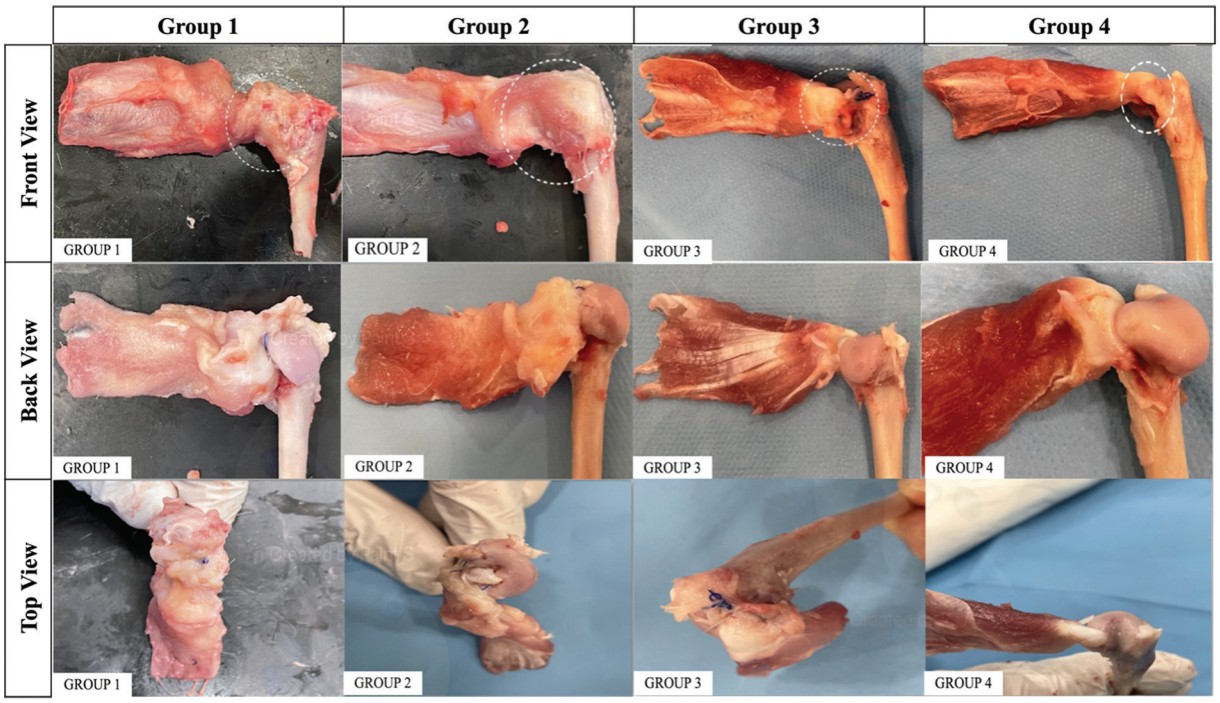

Figure 11. Front, back, and top macroscopic views of the subscapularis tendon-bone unit across groups 1 to 4. The dashed circles indicate the tendon-bone interface regions, highlighting the areas evaluated for scar tissue formation and tendon healing quality.

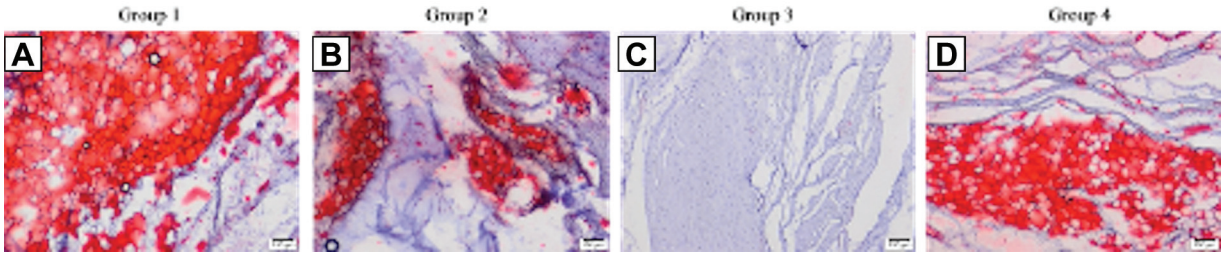

Figure 12. Examination of fat degeneration in (A) group 1, (B) group 2, (C) group 3, and (D) group 4 using Oil Red O staining (scale bar: 100 μm).

in group 3, and negative (–) in group 4 (Figure 15). VEGF immunoreactivity was moderate (++) in group 1, strongly positive (+++) in groups 2 and 3, and negative (–) in group 4. CD31 immunoreactivity was weak (+) in group 1, strongly positive (+++) in group 2, and moderate to strong (++/+++) in group 3 (Figure 15, Table 3).

In addition to statistical significance, group 3 demonstrated histological and biomechanical improvements that may translate into superior clinical outcomes, particularly in terms of reducing fatty degeneration and enhancing collagen organization.

Biomechanics

Biomechanical tensile tests were conducted to evaluate tendon healing quality by analyzing failure mechanisms and load to failure across all groups. Group 4 consisted of intact tendons without surgical intervention, representing the control group and providing baseline biomechanical data for comparison. Two types of tendon failure were observed: insertion tears (failure at the tendon-bone junction) and midsubstance tears (failure within the tendon). A higher rate of midsubstance tear indicates a stronger tendon-to-bone interface, as the repaired site withstands higher forces, leading to rupture occurring within the tendon substance rather than at the repair site. The highest incidence of midsubstance tears was observed equally in group 3 (CGF+SVF scaffold treatment) and the intact control tendons of group 4 (both 85.7%), followed by group 2 (CGF alone; 71.4%), with the lowest rate in group 1 (hydrogel; 28.6%), demonstrating a statistically significant difference among groups (P = .002; Table 4).

TABLE 1
Results Based on Histopathological Scoring Systems[a]

Parameter	Grade	Group 1	Group 2	Group 3	Group 4	*P*	Effect Size (Cohen *w*)
Fatty degeneration						**.045**	0.90
	Grade 1	0 (0.0)	2 (28.6)	4 (57.1)	0 (0.0)		
	Grade 2	2 (28.6)	4 (57.1)	3 (42.8)	0 (0.0)		
	Grade 3	4 (57.1)	1 (14.3)	0 (0.0)	0 (0.0)		
	Grade 4	1 (14.3)	0 (0.0)	0 (0.0)	7 (100.0)		
Vascularity						**.024**	0.74
	Grade 1	3 (42.8)	0 (0.0)	0 (0.0)	7 (100.0)		
	Grade 2	2 (28.6)	2 (28.6)	1 (14.3)	0 (0.0)		
	Grade 3	1 (14.3)	3 (42.8)	1 (14.3)	0 (0.0)		
	Grade 4	1 (14.3)	2 (28.6)	5 (71.4)	0 (0.0)		
Cellularity						**.004**	0.81
	Grade 1	4 (57.1)	0 (0.0)	0 (0.0)	7 (100.0)		
	Grade 2	2 (28.6)	2 (28.6)	0 (0.0)	0 (0.0)		
	Grade 3	1 (14.3)	4 (57.1)	2 (28.6)	0 (0.0)		
	Grade 4	0 (0.0)	1 (14.3)	5 (71.4)	0 (0.0)		
Regularity of collagen fibers						**.006**	0.99
	Grade 1	3 (42.8)	0 (0.0)	0 (0.0)	7 (100.0)		
	Grade 2	4 (57.1)	2 (28.6)	0 (0.0)	0 (0.0)		
	Grade 3	0 (0.0)	3 (42.8)	1 (14.3)	0 (0.0)		
	Grade 4	0 (0.0)	2 (28.6)	6 (85.7)	0 (0.0)		
Continuity of collagen fibers						**.003**	0.91
	Grade 1	4 (57.1)	0 (0.0)	0 (0.0)	7 (100.0)		
	Grade 2	2 (28.6)	1 (14.3)	0 (0.0)	0 (0.0)		
	Grade 3	1 (14.3)	4 (57.1)	2 (28.6)	0 (0.0)		
	Grade 4	0 (0.0)	2 (28.6)	5 (71.4)	0 (0.0)		

[a]Data are presented as n (%). Bold *P* values indicate statistical significance ($P < .05$).

TABLE 2
Values of Histological Grade Parameters Across Groups[a]

	Group 1	Group 2	Group 3	Group 4	*P*
Fatty Degeneration	3 (2-3)	2 (1-2)	1 (1-2)	4 (4-4)	.045
Vascularity	2 (1-3)	3 (2-4)	4 (3-4)	1 (1-1)	.024
Cellularity	1 (1-2)	3 (2-3)	4 (3-4)	1 (1-1)	.004
Regularity of collagen fibers	2 (1-2)	3 (2-4)	4 (4-4)	1 (1-1)	.006
Continuity of collagen fibers	1 (1-2)	3 (3-4)	4 (3-4)	1 (1-1)	.003

[a]Data are presented as median (IQR). *P* values indicate statistical differences between groups.

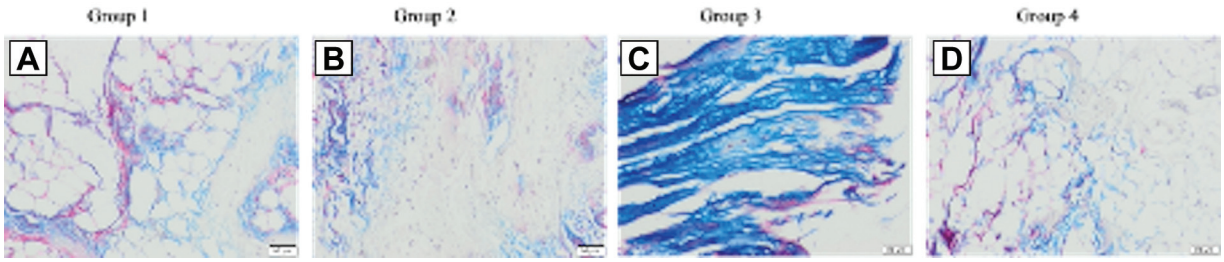

Figure 13. Examination of collagen architecture in sections stained using Masson trichrome staining technique for (A) group 1, (B) group 2, (C) group 3, and (D) group 4 (scale bar: 100 μm).

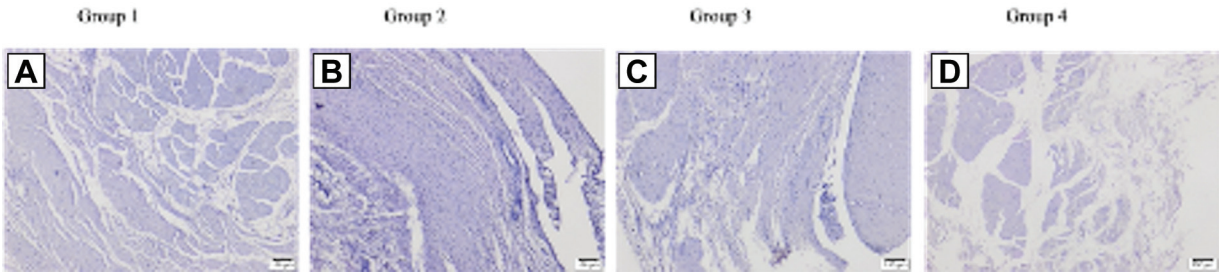

Figure 14. Examination of cellularity and vascularity in (A) group 1, (B) group 2, (C) group 3, and (D) group 4 with hematoxylin-eosin staining (scale bar: 100 μm).

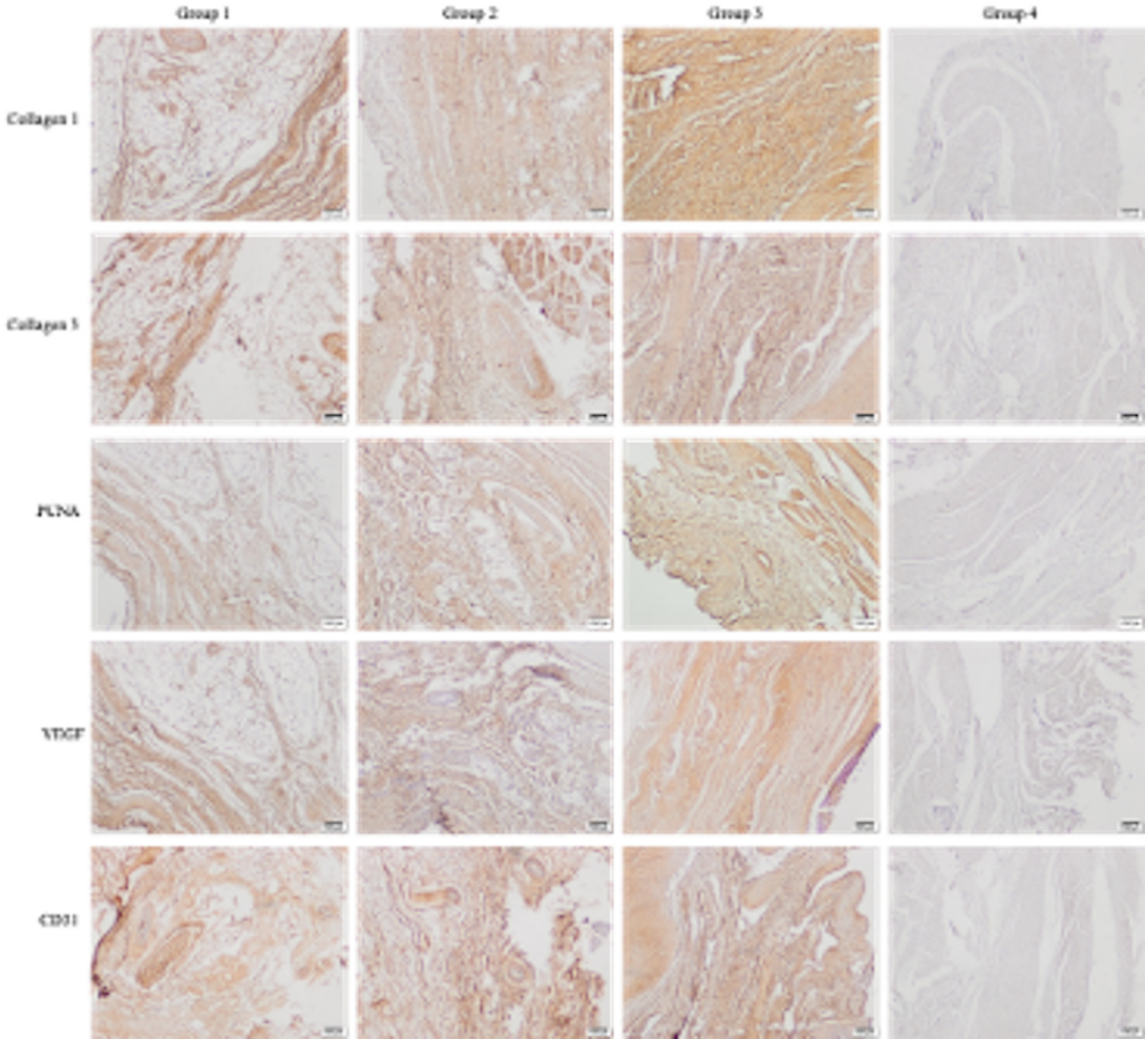

Figure 15. Immunohistochemical staining for type I collagen, type III collagen, vascular endothelial growth factor, proliferating cell nuclear antigen, and cluster of differentiation 31 in groups 1, 2, 3, and 4 (scale bar: 100 μm).

Load-to-failure tests measured the maximal tensile force (in N) that tendons could sustain before rupture. Ultimate tensile strength (load-to-failure) measurements, defined as the maximal force sustained by tendons until rupture, revealed progressive improvements across treatment groups. Group 1 showed the lowest strength (86.57 ± 3.85 N), while group 2 (100.00 ± 6.85 N) and group 3 (116.14 ± 8.49 N) exhibited significant increases. The

TABLE 3
Immunohistochemical Evaluation Scores Across Groups[a]

	Type I Collagen	Type III Collagen	PCNA	VEGF	CD31
Group 1	+/++	+++	+/++	++	+
Group 2	++	++	++	+++	+++
Group 3	+++	++	+++	+++	++/+++
Group 4	–	–	–	–	–

[a]CD31, cluster of differentiation 31; PCNA, proliferating cell nuclear antigen; VEGF, vascular endothelial growth factor. Negative (–), weak (+), moderate (++), strong (+++).

TABLE 4
Biomechanical Evaluation Results Showing Failure Mechanisms and Ultimate Tensile Strength (Load-to-Failure) Across Groups[a]

Parameter	Group 1	Group 2	Group 3	Group 4	*P*
Tensile test result					
Insertion tear (failure at tendon-bone junction)	5 (71.4)	2 (28.6)	1 (14.3)	1 (14.3)	**.002**[b]
Midsubstance tear (failure within tendon)	2 (28.6)	5 (71.4)	6 (85.7)	6 (85.7)	**.002**
Ultimate tensile strength (load-to-failure, N)	86.57 ± 3.85	100.00 ± 6.85	116.14 ± 8.49	122.86 ± 9.57	**<.001**[c]

[a]Data are presented as n (%) or mean ± SD. The bold *P* values indicate statistical significance at $P < .05$.
[b]Pearson chi-square test.
[c]Kruskal-Wallis test.

intact tendons of group 4, representing physiological conditions, showed the highest ultimate tensile strength (122.86 ± 9.57 N), serving as a reference for optimal tendon integrity and physiological benchmark. Statistically significant differences were found among all groups ($P < .001$), except between groups 3 and 4. These findings indicate that tendons treated with the CGF+SVF scaffold achieved biomechanical properties closely comparable with intact tendons (group 4), confirming the effectiveness of CGF+SVF in enhancing tendon repair strength (Table 4, Figures 16 and 17).

DISCUSSION

Our results suggest that CGF+SVF significantly enhances tendon repair by improving vascularity, cellularity, and collagen organization while reducing fatty degeneration and scar tissue. This approach may offer a promising solution for chronic RC repair. Preserving the natural tendon-bone transition region is crucial in the repair of RCT to mitigate mechanical alterations and enhance repair effectiveness. Fibrous scar tissue, characterized histologically by fewer cellular and disorganized fibers, exhibits low strength and fails to replicate the properties of the natural tendon-bone junction.[46]

Liu et al[21] reported that combining SVF and PRP was more effective in promoting wound healing, collagen deposition, angiogenesis, and neuroregeneration in the treatment of pressure ulcers in rats than using these components alone. The study also found that the degradation of growth factors was prolonged when SVF and PRP were combined.

Following RCT formation, cytokines are secreted, attracting inflammatory cells to the injury site and activating the inflammatory cascade. This process induces apoptosis in muscle fibers and at the musculotendinous junction, resulting in degenerative changes. Over time, there is a loss of sarcomeres and muscle atrophy, enlarging the intra- and intermyofibrillary spaces. If the tendon remains unrepaired and retracted, muscle progenitor cells are reprogrammed to enter the adipogenic pathway, transforming into mature adipocytes. These adipocytes infiltrate free myofibrils and the interstitial spaces, leading to fatty degeneration,[46] which may negatively affect inflammation, oxidative stress, and other factors.[30] Khair et al[18] found that postoperative clinical scores were lower in patients with increased fat infiltration following RC repair. Conversely, Oh et al[25] observed reduced fatty degeneration in ADSC recipients compared with saline recipients. Our findings showed the lowest fatty degeneration in the groups treated with CGF+SVF and CGF, consistent with existing literature.

In cases where RCT repair fails to achieve improvement, decreased blood flow due to age-related degeneration and/or hypovascularity resulting from RC damage is observed. Reduced blood flow is considered a poor prognostic marker for RCT healing.[19] Cervelli et al[6] reported that combining PRP and SVF stimulates angiogenesis. Similarly, Okonkwo and DiPietro[26] demonstrated that PRP+SVF enhanced healing in diabetic wounds by

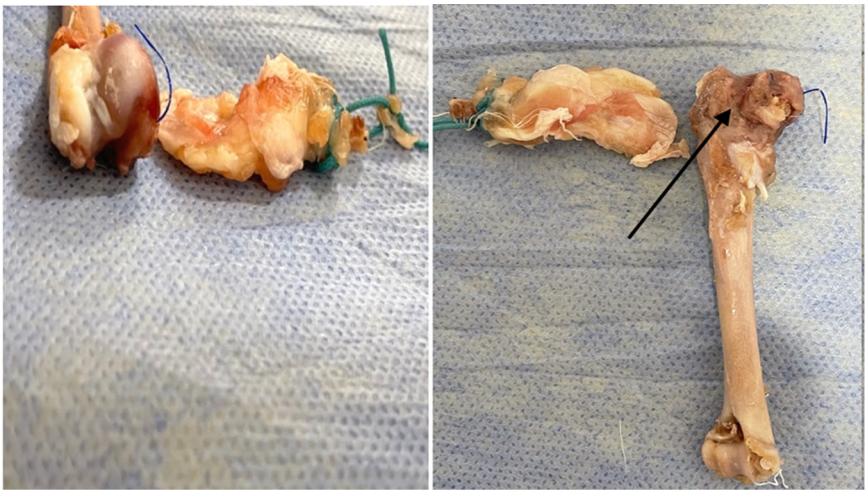

Figure 16. Macroscopic view of the insertion zone tear (black arrow in right panel indicates insertion zone).

Figure 17. Macroscopic view of the midsubstance tear (black arrow in left panel indicates midsubstance of the tendon).

promoting greater neovascularization compared with monotherapies. Our study observed better vascularization and healing in groups 2 and 3, treated with CGF, compared with the repair-only group.

Preventing reactive scar tissue formation can be achieved by enhancing cell differentiation in the RC region associated with the tear.[5] Using stem cells, such as ADSCs, is appealing due to their ability to differentiate into multiple cell types and their potent immunomodulatory properties.[34] Awad et al[2] reported the successful development of tendon structure in a rabbit model using mesenchymal stem cells derived from autologous bone marrow 4 weeks after patellar tendon injury. The study found that CGF fibrin gel and SVF use significantly increased cellularity. Although the direct association between cellularity and improvement is unclear, these results suggest a contribution to the repair process.

Type III collagen deposition and the nonparallel arrangement of these fibers peak 6 to 8 weeks after injury, with healing typically occurring through the formation of macroscopic scar tissue.[42] The higher amount of type III collagen in scar tissue compared with type I collagen results in a relatively weak healing region, increasing the risk of tears at that site.[42] Wang et al[41] reported in a murine model that intravenous injection of adipose exosomes increased the conversion of type III collagen to type I collagen and reduced scar size. In our study, CGF+SVF recipients showed the most favorable results regarding scar tissue formation. The CGF group demonstrated better results than the hydrogel-only group. However, the regularity of collagen fibers was significantly higher in patients using CGF+SVF compared with the other groups. Additionally, while type III collagen immunoreactivity was lower in the CGF and CGF+SVF

groups, type I collagen immunoreactivity, which reduces scar tissue formation, was strongly positive in groups 2 and 3. The addition of SVF+CGF fibrin gel to RCT repair appears to increase the conversion of type III collagen to type I collagen, resulting in less scar tissue and a more regular formation of collagen fibers.

In biomechanical tests, midsubstance tears indicate robust tendon healing and adhesion to the bone, while tears at the tendon's insertion site to the bone suggest poor bone-tendon healing. In line with our biomechanical findings, our tests showed the highest rate of midsubstance tears in the intact tendons of the control group with the highest rate among the treatment groups seen in patients treated with CGF+SVF. This suggests that the CGF+SVF treatment enhances tendon healing to a degree that mimics the failure characteristics of native, uninjured tendons. In Oh et al's[25] study, midsubstance rupture was more frequent in ADSC recipients compared with saline recipients. Similarly, in our study, midsubstance tears were more frequent in the CGF+SVF group, indicating that these scaffolds provide the most favorable biomechanical results for tendon healing.

A study conducted in a rabbit model reported improved mechanical properties of tendons following ADSC injection for patellar tendon rupture (at 6-12 weeks).[35] Awad and colleagues[2] demonstrated that mesenchymal stem cells obtained from autologous bone marrow in a rabbit model increased patellar tendon strength in biomechanical studies 4 weeks postinjury. In a rabbit Achilles tendon rupture model by Uysal et al,[38] the maximal tensile load of the tendon was significantly higher with ADSC+PRP compared with PRP alone. Evaluating tendon durability showed stronger tendon-to-bone adhesion and increased tensile strength from group 1 to 4. These results indicate that tendon healing is more effective with CGF+SVF, as the tendon strength values in group 3 were comparable with those of intact tendons.

Despite substantial evidence from animal studies, the use of biological materials for treating RCTs in humans remains in its early stages. Several studies have shown that stem cell therapy using bone marrow or adipose tissue–derived stem cells is associated with a lower retear rate and reduced pain levels in patients with RCT.[17,20,24,43] Additionally, a study involving 14 RCT patients reported that injecting autologous bone marrow mononuclear cells during transosseous repair via mini-open incision improved tendon tissue quality.[11]

When examining ADSC and PRP studies in the literature, it is common to inject prepared biological material concentrates into the relevant anatomic region. However, the exact amount of injected agent reaching the injury site is often unclear. An alternative approach involves administering biological augmentation in liquid form between the tendon and bone, but this can lead to material loss during the repair process. In the current study, injections were avoided due to the risk of injection-related resistance in the chronic tendon rupture model and the potential for the administered biomaterial to leak outside the tendon area. Additionally, the required biomaterial concentration for tissue-level efficacy remains unclear, leading to a lack of standardization in practice.

We utilized a standard transosseous repair technique and created bone tunnels for reproducible placement of agents, ensuring controlled delivery of the biological agent. The solid application of biological material may contribute to the literature by enhancing the standardization and applicability of the technique. Furthermore, placing the biomaterial in the bone tunnel may stimulate endogenous mesenchymal stem cells and accelerate tissue healing by infiltrating stem cells or growth factors into the bone.

While the results of this study indicate significant therapeutic potential for CGF and SVF enriched fibrin scaffolds in a preclinical model, translating these findings into clinical practice involves notable challenges and risks that must be addressed. These considerations are critical to ensuring the safety and efficacy of the procedure when applied to humans.

A key concern in human applications is the risk of immunological and inflammatory reactions. Although SVF are autologous, variations in cell quality and immunogenicity between individuals may lead to adverse immune responses. Even in autologous applications, mild inflammatory reactions can occur due to contamination during isolation or unintended activation of immune pathways.[10,44]

Another major risk is the potential for tumorigenicity and aberrant differentiation. Stem cell–based therapies carry the risk of uncontrolled differentiation, which may result in complications such as ectopic tissue formation or ossification. Experimental studies have reported cases of such outcomes, highlighting the necessity for stringent protocols to regulate cell behavior.[16]

The technical challenges of delivering and retaining fibrin scaffolds at the site of injury in humans are also significant. In the dynamic mechanical environment of the shoulder joint, scaffold migration or degradation could undermine therapeutic efficacy. Optimizing scaffold composition to improve adhesion and stability is critical to overcoming these challenges.[23] While this study demonstrates short-term benefits, the potential long-term effects, such as scaffold biodegradation, changes in biomechanical properties, and fibrosis, require further investigation.

Limitations

This study has several limitations. It was conducted using an animal model, with the chronic RCT model created by the researcher. While this study provides valuable insights, its limitations include the use of a single tendon injury model, which may not fully replicate the complexity of human RC injuries involving multiple tendons.

Dynamic analyses were not performed on the RC muscle, which could have provided further insights into the functional strength of the muscle. The inclusion of additional functional tests, such as electromyography, could have enhanced our understanding of the effects of CGF and SVF on the RC muscle.

Despite these limitations, our study presents promising results that could inform the development of standardized treatment approaches using CGF and SVF as solid fibrin scaffolds for the surgical repair of RCTs. Further research

is necessary to validate and expand upon our findings and to develop standardized protocols for the preparation and application of CGF and SVF.

CONCLUSION

The application of CGF and/or SVF during the surgical repair of chronic RCTs shows promise in improving outcomes by reducing fatty degeneration and scar tissue and enhancing collagen fiber organization, vascularity, cellularity, and tendon strength. These effects were most pronounced with the combination of CGF and SVF in a fibrin scaffold. Future clinical trials are needed to confirm these findings and evaluate their applicability in human patients.

ORCID iDs

Ahmet Keskin https://orcid.org/0000-0001-8627-5651
Serhat Gurbuz https://orcid.org/0000-0002-6120-3325
Bülent Karslioğlu https://orcid.org/0000-0001-6127-9672

REFERENCES

1. A Hamid MS, Sazlina SG. Platelet-rich plasma for rotator cuff tendinopathy: a systematic review and meta-analysis. *PLoS One*. 2021;16(5):e0251111. doi:10.1371/journal.pone.0251111
2. Awad HA, Butler DL, Boivin GP, et al. Autologous mesenchymal stem cell-mediated repair of tendon. *Tissue Eng*. 1999;5(3):267-277. doi:10.1089/ten.1999.5.267
3. Behfar M, Sarrafzadeh-Rezaei F, Hobbenaghi R, Delirezh N, Dalir-Naghadeh B. Adipose-derived stromal vascular fraction improves tendon healing in rabbits. *Chin J Traumatol*. 2011;14(6):329-335.
4. Berebichez-Fridman R, Gómez-García R, Granados-Montiel J, et al. The holy grail of orthopedic surgery: mesenchymal stem cells—their current uses and potential applications. *Stem Cells Int*. 2017;2017:2638305. doi:10.1155/2017/2638305
5. Cai J, Xu J, Ye Z, et al. Exosomes derived from kartogenin-preconditioned mesenchymal stem cells promote cartilage formation and collagen maturation for enthesis regeneration in a rat model of chronic rotator cuff tear. *Am J Sports Med*. 2023;51(5):1267-1276. doi:10.1177/03635465231155927
6. Cervelli V, Bocchini I, Di Pasquali C, et al. P.R.L. Platelet rich lipotransfert: our experience and current state of art in the combined use of fat and PRP. *Biomed Res Int*. 2013;2013:434191. doi:10.1155/2013/434191
7. Chung SW, Song BW, Kim YH, Park KU, Oh JH. Effect of platelet-rich plasma and porcine dermal collagen graft augmentation for rotator cuff healing in a rabbit model. *Am J Sports Med*. 2013;41(12):2909-2918. doi:10.1177/0363546513503810
8. Condron NB, Kester BS, Tokish JM, et al. Nonoperative and operative soft-tissue, cartilage, and bony regeneration and orthopaedic biologics of the shoulder: an Orthoregeneration Network (ON) Foundation review. *Arthroscopy*. 2021;37(10):3200-3218. doi:10.1016/j.arthro.2021.06.033
9. Corigliano M, Sacco L, Baldoni E. CGF—una proposta terapeutica per la medicina rigenerativa. *Odontoiatria*. 2010;1:69-81.
10. Desgres M, Menasché P. Clinical translation of pluripotent stem cell therapies: challenges and considerations. *Cell Stem Cell*. 2019;25(5):594-606. doi:10.1016/j.stem.2019.10.001
11. Ellera Gomes JL, da Silva RC, Silla LM, Abreu MR, Pellanda R. Conventional rotator cuff repair complemented by the aid of mononuclear autologous stem cells. *Knee Surg Sports Traumatol Arthrosc*. 2012;20(2):373-377. doi:10.1007/s00167-011-1607-9
12. Frey E, Regenfelder F, Sussmann P, et al. Adipogenic and myogenic gene expression in rotator cuff muscle of the sheep after tendon tear. *J Orthop Res*. 2009;27(4):504-509. doi:10.1002/jor.20695
13. Ghidoni I, Chlapanidas T, Bucco M, et al. Alginate cell encapsulation: new advances in reproduction and cartilage regenerative medicine. *Cytotechnology*. 2008;58(1):49-56. doi:10.1007/s10616-008-9161-0
14. Grumet RC, Hadley S, Diltz MV, Lee TQ, Gupta R. Development of a new model for rotator cuff pathology: the rabbit subscapularis muscle. *Acta Orthop*. 2009;80(1):97-103. doi:10.1080/17453670902807425
15. Han J, Han SC, Kim YK, et al. Bioactive scaffold with spatially embedded growth factors promotes bone-to-tendon interface healing of chronic rotator cuff tear in rabbit model. *Am J Sports Med*. 2023;51(9):2431-2442. doi:10.1177/03635465231180289
16. Harris MT, Butler DL, Boivin GP, Florer JB, Schantz EJ, Wenstrup RJ. Mesenchymal stem cells used for rabbit tendon repair can form ectopic bone and express alkaline phosphatase activity in constructs. *J Orthop Res*. 2004;22(5):998-1003. doi:10.1016/j.orthres.2004.02.012
17. Hurd JL, Facile TR, Weiss J, et al. Safety and efficacy of treating symptomatic, partial-thickness rotator cuff tears with fresh, uncultured, unmodified, autologous adipose-derived regenerative cells (UA-ADRCs) isolated at the point of care: a prospective, randomized, controlled first-in-human pilot study. *J Orthop Surg Res*. 2020;15(1):122. doi:10.1186/s13018-020-01631-8
18. Khair MM, Lehman J, Tsouris N, Gulotta LV. A systematic review of preoperative fatty infiltration and rotator cuff outcomes. *HSS J*. 2016;12(2):170-176. doi:10.1007/s11420-015-9465-5
19. Kim SH, Cho WS, Joung HY, Choi YE, Jung M. Perfusion of the rotator cuff tendon according to the repair configuration using an indocyanine green fluorescence arthroscope: a preliminary report. *Am J Sports Med*. 2017;45(3):659-665. doi:10.1177/0363546516669778
20. Kim SJ, Kim EK, Kim SJ, Song DH. Effects of bone marrow aspirate concentrate and platelet-rich plasma on patients with partial tear of the rotator cuff tendon. *J Orthop Surg Res*. 2018;13(1):1. doi:10.1186/s13018-017-0693-x
21. Liu Z, Xiao S, Tao K, et al. Synergistic effects of human platelet-rich plasma combined with adipose-derived stem cells on healing in a mouse pressure injury model. *Stem Cells Int*. 2019;2019:3091619. doi:10.1155/2019/3091619
22. Lu LY, Kuang CY, Yin F. Magnetic resonance imaging and biomechanical analysis of adipose-derived stromal vascular fraction applied on rotator cuff repair in rabbits. *Chin Med J (Engl)*. 2018;131(1):69-74. doi:10.4103/0366-6999.221264
23. Mazzocca AD, McCarthy MB, Chowaniec DM, Cote MP, Arciero RA, Drissi H. Rapid isolation of human stem cells (connective tissue progenitor cells) from the proximal humerus during arthroscopic rotator cuff surgery. *Am J Sports Med*. 2010;38(7):1438-1447. doi:10.1177/0363546509360924
24. Mirghaderi SP, Valizadeh Z, Shadman K, et al. Cell therapy efficacy and safety in treating tendon disorders: a systemic review of clinical studies. *J Exp Orthop*. 2022;9(1):85. doi:10.1186/s40634-022-00520-9
25. Oh JH, Chung SW, Kim SH, Chung JY, Kim JY. 2013 Neer Award: effect of the adipose-derived stem cell for the improvement of fatty degeneration and rotator cuff healing in rabbit model. *J Shoulder Elbow Surg*. 2014;23(4):445-455. doi:10.1016/j.jse.2013.07.054
26. Okonkwo UA, DiPietro LA. Diabetes and wound angiogenesis. *Int J Mol Sci*. 2017;18(7):1419. doi:10.3390/ijms18071419
27. Rodella LF, Favero G, Boninsegna R, et al. Growth factors, CD34 positive cells, and fibrin network analysis in concentrated growth factors fraction. *Microsc Res Tech*. 2011;74(8):772-777. doi:10.1002/jemt.20968
28. Roßbach BP, Gülecyüz MF, Kempfert L, et al. Rotator cuff repair with autologous tenocytes and biodegradable collagen scaffold: a histological and biomechanical study in sheep. *Am J Sports Med*. 2020;48(2):450-459. doi:10.1177/0363546519892580
29. Rubino LJ, Stills HF Jr, Sprott DC, Crosby LA. Fatty infiltration of the torn rotator cuff worsens over time in a rabbit model. *Arthroscopy*. 2007;23(7):717-722. doi:10.1016/j.arthro.2007.01.023

30. Samadi A, Sabuncuoglu S, Samadi M, et al. A comprehensive review on oxysterols and related diseases. *Curr Med Chem*. 2021;28(1):110-136. doi:10.2174/0929867327666200316142659
31. Seida JC, LeBlanc C, Schouten JR, et al. Systematic review: nonoperative and operative treatments for rotator cuff tears. *Ann Intern Med*. 2010;153(4):246-255. doi:10.7326/0003-4819-153-4-201008170-00263
32. Song W, Zhang D, Wu D, et al. Cryopreserved adipose-derived stem cell sheets: an off-the-shelf scaffold for augmenting tendon-to-bone healing in a rabbit model of chronic rotator cuff tear. *Am J Sports Med*. 2023;51(8):2005-2017. doi:10.1177/03635465231171682
33. Song Y, Li P, Xu Y, Lin Z, Deng Z, Chen C. Menstrual blood–derived mesenchymal stem cells encapsulated in autologous platelet-rich gel facilitate rotator cuff healing in a rabbit model of chronic tears. *Am J Sports Med*. 2023;51(7):1872-1885. doi:10.1177/03635465231168104
34. Steinert AF, Rackwitz L, Gilbert F, Nöth U, Tuan RS. Concise review: the clinical application of mesenchymal stem cells for musculoskeletal regeneration: current status and perspectives. *Stem Cells Transl Med*. 2012;1(3):237-247. doi:10.5966/sctm.2011-0036
35. Taylor MA, Norman TL, Clovis NB, Blaha JD. The response of rabbit patellar tendons after autologous blood injection. *Med Sci Sports Exerc*. 2002;34(1):70-73. doi:10.1097/00005768-200201000-00012
36. Trudel G, Ramachandran N, Ryan SE, Rakhra K, Uhthoff HK. Supraspinatus tendon repair into a bony trough in the rabbit: mechanical restoration and correlative imaging. *J Orthop Res*. 2010;28(6):710-715. doi:10.1002/jor.21045
37. Uhthoff HK, Seki M, Backman DS, Trudel G, Himori K, Sano H. Tensile strength of the supraspinatus after reimplantation into a bony trough: an experimental study in rabbits. *J Shoulder Elbow Surg*. 2002;11(5):504-509. doi:10.1067/mse.2002.126760
38. Uysal CA, Tobita M, Hyakusoku H, Mizuno H. Adipose-derived stem cells enhance primary tendon repair: biomechanical and immunohistochemical evaluation. *J Plast Reconstr Aesthet Surg*. 2012;65(12):1712-1719. doi:10.1016/j.bjps.2012.06.011
39. Wang C, Hu Q, Song W, Yu W, He Y. Adipose stem cell–derived exosomes decrease fatty infiltration and enhance rotator cuff healing in a rabbit model of chronic tears. *Am J Sports Med*. 2020;48(6):1456-1464. doi:10.1177/0363546520908847c
40. Wang C, Zhang Y, Zhang G, Yu W, He Y. Adipose stem cell–derived exosomes ameliorate chronic rotator cuff tendinopathy by regulating macrophage polarization: from a mouse model to a study in human tissue. *Am J Sports Med*. 2021;49(9):2321-2331. doi:10.1177/03635465211020010
41. Wang L, Hu L, Zhou X, et al. Exosomes secreted by human adipose mesenchymal stem cells promote scarless cutaneous repair by regulating extracellular matrix remodelling. *Sci Rep*. 2017;7(1):13321. doi:10.1038/s41598-017-12919-x
42. Zhang X, Cai Z, Wu M, Huangfu X, Li J, Liu X. Adipose stem cell–derived exosomes recover impaired matrix metabolism of torn human rotator cuff tendons by maintaining tissue homeostasis. *Am J Sports Med*. 2021;49(4):899-908. doi:10.1177/0363546521992469
43. Zhang X, Han Z, Han K, et al. Loading mesenchymal stem cell–derived exosomes into a traditionally designed rotator cuff patch: a potential strategy to enhance the repair of chronic rotator cuff tear associated with degenerative changes. *Am J Sports Med*. 2022;50(8):2234-2246. doi:10.1177/03635465221096490
44. Zhang Y, Ju W, Zhang H, Mengyun L, Shen W, Chen X. Mechanisms and therapeutic prospects of mesenchymal stem cells-derived exosomes for tendinopathy. *Stem Cell Res Ther*. 2023;14(1):307. doi:10.1186/s13287-023-03431-3
45. Zuk PA, Zhu M, Mizuno H, et al. Multilineage cells from human adipose tissue: implications for cell-based therapies. *Tissue Eng*. 2001;7(2):211-228. doi:10.1089/107632701300062859
46. Zumstein MA, Lädermann A, Raniga S, Schär MO. The biology of rotator cuff healing. *Orthop Traumatol Surg Res*. 2017;103(1)(suppl):S1-S10. doi:10.1016/j.otsr.2016.11.003